

1 Influence of Surface Texture and Acid–Base Properties on Ozone
2 Decomposition Catalyzed by Aluminum (Hydroxyl) Oxides

3
4 Fei Qi ^a, Zhonglin Chen ^{a*}, Bingbing Xu ^a, Jimin Shen ^a, Jun Ma ^a, Cynthia Joll ^b,
5 Anna Heitz ^b

6 ^a State Key Laboratory of Urban Water Resource and Environment, School of
7 Municipal & Environmental Engineering, the Second campus, Harbin Institute of
8 Technology, P.O. Box 2606, Harbin 150090, China

9 Email: qifei_hit@yahoo.com.cn; zhonglinchen@263.net; xbb_hit@126.com;
10 sjm1973@sohu.com; majun_hit@163.com

11
12 * Corresponding author: Zhonglin Chen

13 Email: zhonglinchen@263.net;

14 Tel.: +86-451-86283028 Fax: +86-451-86283028

15
16 ^b Curtin Water Quality Research Centre, Curtin University of Technology, BENTLEY
17 WA 6102, Australia

18 Email: c.joll@curtin.edu.au; a.heizt@curtin.edu.au

23 ABSTRACT

24 The decomposition of aqueous ozone in the presence of three aluminum (hydroxyl)
25 oxides was studied, respectively. It was hypothesized that surface hydroxyl groups
26 and acid-base properties of aluminum (hydroxyl) oxides play an important role in
27 catalyzed ozone decomposition. The variables investigated were oxide dose, aqueous
28 pH, presence of inorganic anions (sulfate and nitrate), the effect of tert-butyl alcohol
29 (TBA) and surface hydroxyl groups density of the three aluminum (hydroxyl) oxides.
30 All three aluminum (hydroxyl) oxides tested, i.e. γ -AlOOH (HAO), γ -Al₂O₃ (RAO)
31 and α -Al₂O₃ (AAO), enhanced the rate of ozone decomposition. The net surface
32 charge of the aluminum (hydroxyl) oxides favored in catalyzed ozone decomposition.
33 The greatest effect on catalyzed ozone decomposition was observed when the solution
34 pH was close to the point of zero charge of the aluminum (hydroxyl) oxide. Sulfate
35 and nitrate were substituted for the surface hydroxyl groups of the aluminum
36 (hydroxyl) oxides, which then complexed with Al³⁺ in a ligand exchange reaction.
37 Therefore, inorganic anions may be able to inhibit catalyzed ozone decomposition. It
38 was confirmed that surface hydroxyl groups were important for ozone decomposition
39 with aluminum (hydroxyl) oxides as catalysts. TBA inhibited ozone decomposition in
40 the presence of HAO, RAO and AAO. It was also tested whether aluminum (hydroxyl)
41 oxides catalyzed ozone-transformed hydroxyl radicals. The relationship between
42 surface hydroxyl groups and the ratio of hydroxyl radical concentration to ozone
43 concentration (R_{ct}) was investigated quantitatively. Higher density of surface hydroxyl
44 groups of the aluminum oxide tested was favorable for the decay of ozone into

45 hydroxyl radicals.

46

47 Keywords: aluminum (hydroxyl) oxide; acid-base property; point of zero charge;

48 surface hydroxyl group; hydroxyl radical

49

50

51

52

53

54

55

56

57

58

59

60

61

62

63

64

65

66

67 Abbreviations:

68 TBA tert-butyl alcohol

69 HAO γ -AlOOH

70 RAO γ -Al₂O₃

71 AAO α -Al₂O₃

72 R_{ct} the ratio of hydroxyl radical concentration to ozone concentration

73 PZC point of zero charge

74 pCBA p-chlorobenzoic acid

75 A_{BET} BET surface area (m² g⁻¹)

76 V_{tal} total pore volume (mL g⁻¹)

77 V_{micro} micropore pore volume (mL g⁻¹)

78 D_{avg} average diameter of pore (nm)

79 [O₃] dissolved ozone concentration (mg L⁻¹)

80 [catalyst] catalyst dose (mg L⁻¹)

81 k_{O₃} kinetics rate constant of ozone decomposition alone (min⁻¹)

82 k_{cata} kinetics rate constant of catalyzed ozone decomposition ((mol L)⁻¹ s⁻¹)

83 k_{TBA} apparent kinetics rate constant of catalyzed ozone decomposition within TBA

84 (min⁻¹)

85

86

87

88

89 1. Introduction

90 Ozone is one of the most powerful oxidizing agents available in water treatment [1].

91 Ozone can react fast with organic pollutants including double bonds, aromatic groups,

92 and amino groups [2, 3]. In order to enhance the efficiency of ozonation, Ma et al. [4,

93 5] combined the ozone with homogeneous and heterogeneous catalysts, with or

94 without metallic phases. Catalyzed ozonation is a promising technology for the

95 effective removal from drinking water and wastewater of pollutants that are

96 recalcitrant to conventional water treatments [6]. The main advantages of catalyzed

97 ozonation relative to traditional ozonation are enhanced ozone utilization, increased

98 efficiency of pollutant removal and improved organic matter mineralization [7].

99 Heterogeneous catalytic ozonation, though less studied than the homogeneous process,

100 is more attractive as it provides greater oxidation efficiency, costs less and it is more

101 feasible for practical application. Different supported and unsupported catalysts have

102 been tested in the ozonation of several organic compounds. The heterogeneous

103 catalysts used are usually MnO_2 [8], TiO_2 [9], Al_2O_3 [10, 11], α - $FeOOH$ [12, 13],

104 activated carbon [14- 17], ZnO [18], noble metals [19, 20] and mixed metal oxides

105 [21]. These catalysts were investigated on removal different organic matter in

106 drinking water or wastewater. Different catalytic mechanisms for degradation

107 different organic matter were proposed.

108

109 Aluminum oxides have been used in water treatment technology mainly as an ion

110 exchanger for the removal of inorganic anions such as As and F [22]. The utilization

111 of aluminum oxides as supports for active species, mainly metals and metal oxides, in
112 the catalytic ozonation of several organic compounds was also studied [12]. Alumina
113 was found to be an effective catalyst for the ozonation of 2-chlorophenol and for
114 refractory organic compounds such as oxalic, acetic, salicylic and succinic acids [23,
115 24]. In recent years, researchers have realized that the efficiency of ozonation
116 catalyzed by aluminum oxides is mainly a result of their ability to transform ozone
117 into $\cdot\text{OH}$ radicals, which are the strongest oxidants in water. Although there is
118 agreement that catalysts enhance aqueous ozone decomposition by allowing the
119 formation of $\cdot\text{OH}$ radicals, the mechanism of catalyzed ozone decomposition and the
120 relationship between catalysts and their abilities to catalyze ozone decomposition are
121 still not well understood.

122

123 Due to the special surface characteristics and structure of aluminum oxides, their
124 applications in drinking water and wastewater purification are increasing. When
125 aluminum oxides are introduced into water, they strongly adsorb H_2O molecules.
126 Chemisorption of water onto aluminum oxide surfaces is considered to be a reaction
127 between the Al ion, an electron acceptor (Lewis acid), and the hydroxyl ion, its
128 electron donor (Lewis base). At the same time, acidity and basicity are the two main
129 parameters determining the catalytic properties of aluminum oxides [25].

130

131 The objective of the present work was to study systematically the influence of the
132 surface texture and the acid-base properties of aluminum (hydroxyl) oxides in the

133 catalytic decomposition of ozone in aqueous solution. The behavior of various
134 aluminum (hydroxyl) oxides, including γ -AlOOH (HAO), γ -Al₂O₃ (RAO) and
135 α -Al₂O₃ (AAO), in decomposing aqueous ozone was examined. The influence of the
136 main variables affecting the rate of ozone decomposition (i.e. aluminum oxide dose,
137 solution pH, presence of the OH scavenger tert-butyl alcohol, inorganic anions, as
138 well as structure and acid–base properties of the aluminum (hydroxyl) oxides) were
139 evaluated, thus providing insights into the mechanism of ozonation catalyzed by
140 aluminum oxides.

141

142 2. Experimental

143 2.1 Catalysts and chemicals

144 Catalysts were synthesized in our laboratory. The aluminum oxide γ -AlOOH (HAO)
145 was obtained by precipitating aluminum nitrate with ammonia until pH reached 9.0.
146 The suspension was aged at 30 °C for 10-15 days. Then the precipitate was repeatedly
147 rinsed with deionized water until the conductivity of the supernatant remained
148 constant over three consecutive rinses. The precipitate was further dried at 70 °C. The
149 aluminum oxides γ -Al₂O₃ (RAO) and α -Al₂O₃ were obtained by calcining the HAO at
150 450 °C and 1150 °C for 4 h, respectively. The crystalline phases of the catalysts were
151 confirmed by X-ray diffraction (XRD). The HAO, RAO and AAO were ground and
152 particles with diameters between 0.075 mm and 0.3 mm were used in experiments.
153 All chemicals used were of analytical reagent or higher grade.

154

155 2.2 Analysis

156 2.2.1 Surface texture characterization

157 Surface area, pore volume and average pore size of aluminum (hydroxyl) oxides were
158 obtained on a Surface Area and Porosity Analyzer (Micromeritics ASAP 2020, USA).

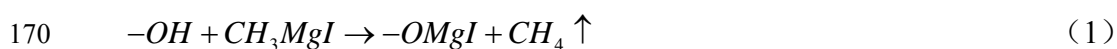
159

160 2.2.2 PZC and density of surface hydroxyl groups

161 The point of zero charge (PZC) was determined using the mass titration method
162 described elsewhere [26]. The titration reagents were HClO₄ and NaOH. The
163 electrolyte used was sodium perchlorate at ionic strengths of 0.005, 0.05 and 0.5
164 mol L⁻¹.

165

166 The density of surface hydroxyl groups was measured by Grignard method, described
167 by Tamura [27]. The surface hydroxyl groups on metal oxides (-OH) react with
168 methyl magnesium iodide (CH₃MgI) to evolve methane according to the following
169 reaction (equation. (1)).



171

172 2.2.3 Aqueous ozone and p-Chlorobenzoic acid (pCBA)

173 The aqueous ozone concentration was measured using the indigo method [28]. The
174 purity of the p-Chlorobenzoic acid (pCBA), which was purchased from Sigma USA,
175 was 98%. A stock solution of pCBA (3.19 mmol L⁻¹) was prepared by dissolving it in
176 distilled water. The concentration of pCBA was analyzed by HPLC (LC-10AVP,

177 Shimadzu, Japan) equipped with UV detection. The chromatograph column used was
178 VP-ODS (Shimadzu, Japan). Samples were analyzed using an eluent (containing 0.5
179 percent H₃PO₄ and methanol in the ratio 7:3) at delivered at 1 mL min⁻¹ and detected
180 at 234 nm. The injection volume was 100 μL.

181

182 2.2.4 Sulfate and nitrate

183 The concentrations of sulfate and nitrate after the adsorption by aluminum oxides
184 were determined by a Dionex ICS-3000 ion chromatography equipped with an IonPac
185 AS II-HC (Dionex, USA) ion-exchange column and a conductivity detector. The
186 eluent was a solution of KOH (30.0 mmol L⁻¹) at a flow rate of 1.2 mL min⁻¹.

187

188 2.3 Experimental procedures

189 Catalyzed ozone decomposition experiments were carried out in batch mode at
190 ambient temperatures (20 ± 2 °C). The glass reactor was a flat-bottomed flask with a
191 volume of 1 L. Ozone gas was generated from dried oxygen using a laboratory ozone
192 generator (DHX-SS-1G, Harbin Electrochemistry Engineering Ltd. China). After the
193 generator reached a steady state, ozone gas was bubbled into distilled water in the
194 reactor with a silica dispenser for a desired period. The initial aqueous ozone
195 concentration was controlled by changing the electrical current of the ozone generator.
196 Then, the ozone gas was shut off when the desired ozone concentration reached. The
197 initial aqueous ozone concentration was 1.69 ± 0.02 mg L⁻¹ for each experiment.
198 Catalysts were quickly introduced into the reactor. The reactor was instantly sealed

199 and the magnetic stirrer was turned on to initiate the catalytic ozone decomposition
200 reaction. Samples were withdrawn at pre-selected reaction times. After the residual
201 ozone was instantly quenched with indigo. The solution pH was adjusted with HClO₄
202 and NaOH when experiments were conducted in distilled water.

203

204 Experiments to determine R_{ct} , the ratio of hydroxyl radical concentration to ozone
205 concentration, were carried out in the reactor described above. Ozone was introduced
206 into the reactor as shown above. The stock solution of pCBA and catalysts were
207 quickly introduced into the reactor. The reactor was instantly sealed and the magnetic
208 stirrer was then turned on to initiate the catalytic ozonation experiments. Samples
209 were collected at pre-selected reaction time and the residual ozone was quenched
210 instantly using a sodium sulfite solution (pre-acidified with sulfuric acid to pH 5).
211 Samples were filtered with cellulose acetate filters (0.45 μ m) and were transferred to
212 25 mL volumetric flasks.

213

214 3. Results and Discussion

215 3.1 Textural characterization and acid-base properties of aluminum (hydroxyl) oxides

216 Textural characteristics of the aluminum (hydroxyl) oxides used in the ozone
217 decomposition experiments were shown in Table 1. RAO had the largest surface area
218 and pore volume of the three aluminum oxides tested. When the aluminum oxides
219 were calcined at 1150 °C, AAO had the lowest surface area and pore volume. The
220 average particle diameter showed remarkable variation. As the calcination

221 temperature increased, the particle diameter of the aluminum oxides increased.

222

223 Table 2 shows the acid-base properties of the aluminum (hydroxyl) oxides. The PZC
224 and the density of surface hydroxyl groups were determined. The PZC of aluminum
225 (hydroxyl) oxides increased as the calcination temperature increased. For HAO, PZC
226 was within the neutral range. For both RAO and AAO, PZC was within the alkaline
227 range. The density of surface hydroxyl groups decreased as the calcination
228 temperature increased. Under conditions of both high temperature and high pressure,
229 surface hydroxyl groups may dehydrate from the oxide surface. AAO still had some
230 surface hydroxyl groups, for calcined at high temperature but not high pressure.

231

232 3.2 First order kinetic model for ozone decomposition and apparent first order kinetic
233 model in the presence of aluminum (hydroxyl) oxides

234 Aqueous ozone decomposition in distilled water follows first order kinetics expressed
235 by equation (2)

$$236 \quad -\frac{d[O_3]}{dt} = k_{O_3}[O_3] \quad (2)$$

237 Aqueous ozone decomposition with catalysts in distilled water follows second order
238 kinetics denoted by equation (3).

$$239 \quad -\frac{d[O_3]}{dt} = k_{cata}[O_3][catalyst] \quad (3)$$

240 During the catalyzed ozone decay process, the concentration of solid catalyst did not
241 change. As $k_{O_3-cata} = k_{cata}[catalyst]$, based on apparent first order kinetics, equation (3)

242 can be modified to create equation (4).

243
$$-\frac{d[O_3]}{dt} = k_{O_3-cata}[O_3] \quad (4)$$

244 Rate constants for the catalyzed decomposition of ozone can be used to indicate the
245 effectiveness of a catalyst. Using these rate constants, the effect of some major
246 variables can be defined exactly. According to equations (2) and (4), rate constants for
247 ozone decomposition and the apparent rate constant for ozone decomposition with
248 aluminum (hydroxyl) oxides could be obtained from the slope of the relationship
249 between $\ln([O_3]/[O_3]_0)$ and reaction time. Figure 1 shows kinetic plots for ozone
250 decomposition with and without catalysts. The plots show an initial phase of ozone
251 disappearance followed by a phase of slower ozone decomposition. This behavior was
252 also observed for ozone decomposition in natural waters and on activated carbon [3,
253 29]. In these cases, the first phase, called instantaneous ozone demand (IOD), was
254 explained by the fast consumption of ozone by natural organic matter in natural
255 waters and by the transformation of ozone into activated oxygen groups by activated
256 carbon, which in turn contributes to the overall ozone consumption. The data for the
257 initial phase (approx. 0–10 min) can be fitted to apparent first order kinetics ($R^2 >$
258 0.99) (Figure 1). Rate coefficients can be obtained for ozone decomposition with
259 aluminum (hydroxyl) oxides. This coefficient can be considered to describe the
260 amount of ozone uptake by HAO, RAO and AAO. Nevertheless, though the
261 application of the first order kinetic model is not a rigorous method, k values obtained
262 from this model were used in this study in order to allow the comparison of the
263 efficiency of the three aluminum (hydroxyl) oxides and to evaluate the influence of
264 several variables on the ozone decomposition rate. Therefore, further discussion will

265 focus mainly on the initial reaction phases.

266

267 A series of ozone decomposition experiments were carried out at constant temperature
268 and solution pH but with varying doses of aluminum (hydroxyl) oxides (0.05–0.4g
269 L⁻¹). In Figure 2 the rate coefficient for ozone decomposition, k_{O_3-cata} , is plotted
270 against the dose of aluminum (hydroxyl) oxides. The ozone decomposition rate was
271 enhanced by an increasing dose of aluminum (hydroxyl) oxides. Over the entire range
272 of doses, the experimental data fit well to a straight line ($R^2 > 0.999$). The slope of the
273 plot was expressed by k_{cata} (Fig. 2).

274

275 Based on these results, ozone decomposition catalyzed by aluminum (hydroxyl)
276 oxides followed second order kinetics with respect to ozone concentration and catalyst
277 dose. Results shown in Figures 1 and 2 confirm the hypothesis of equation (3) and the
278 derivation of equation (4) from equation (3). The observed first order rate constant
279 with respect to ozone concentration for the overall reaction takes into consideration
280 both the heterogeneous reaction taken place on the aluminum (hydroxyl) oxides and
281 the homogeneous reactions taken place in the aqueous phase.

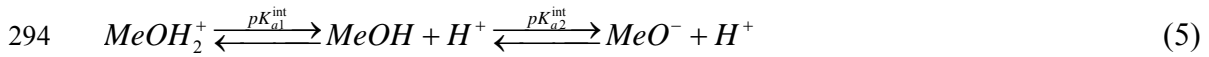
282

283 3.3 Effect of solution pH

284 Solution pH is one of the most important factors in the ozone decomposition process.

285 Hydroxide ions (OH⁻) were found to be the initiator of the chain reaction in ozone
286 decomposition [1]. Solution pH reflected the concentration of OH⁻ in solution. The

287 rate of ozone decomposition increased with increasing pH, which promoted the
 288 formation of OH. Solution pH is also one of the most important factors affecting the
 289 surface properties of oxides [25]. The surface charges of the metal oxides achieved
 290 proton balance. When the net surface charge was zero, the pH of the solution was
 291 PZC. Equation (5) shows the proton balance equation of metal oxides. Under acidic
 292 conditions (pH < PZC), the surfaces of metal oxides are electropositive, while under
 293 basic conditions (pH > PZC), the surfaces of metal oxides are electronegative.



295 The effect of solution pH on the rate of ozone decomposition was studied by
 296 analyzing the ozone decomposition reaction constant. The aim of this investigation
 297 was to elucidate the effects of solution pH and of the surface charge of aluminum
 298 (hydroxyl) oxides on catalyzed ozone decomposition. In Figure 3, the X-axis denotes
 299 the pH, while the Y-axis shows the reaction rate constant of catalyzed ozone
 300 decomposition minus the rate of uncatalyzed ozone decomposition ($k_{O_3-cata} - k_{O_3}$). The
 301 values for ($k_{O_3-cata} - k_{O_3}$) in Figure 3 indicate the contribution of the catalysts to ozone
 302 decomposition. There was an inflexion in the response curves of each of HAO, RAO
 303 and AAO. The inflexions appeared when pH was 7.0, 8.77 and 9.0 for HAO, RAO
 304 and AAO, respectively. These inflexions show the maximum impact of the catalysts
 305 over the pH range 2–11. That is, when solution pH was 7.0, 8.77 and 9.0, HAO, RAO
 306 and AAO had the greatest effect on enhancing ozone decomposition. The PZC for
 307 each of the aluminum (hydroxyl) oxides were 7.26, 8.26 and 9.40 (Table 2), that is,
 308 close to the inflexion in the response curve of each of the oxides. It was concluded

309 that when solution pH was close to PZC of the aluminum (hydroxyl) oxides, the
310 oxides exhibited maximum effect on ozone decomposition. Therefore, zero charge
311 surfaces of aluminum (hydroxyl) oxides and their surface hydroxyl groups were more
312 active than electropositive or electronegative surfaces in catalyzing ozone
313 decomposition.

314

315 3.4 Effect of the presence of inorganic anions

316 In relation to the effect of pH on catalyzed ozone decomposition in the presence of
317 HAO, RAO and AAO, the activity of aluminum (hydroxyl) oxides in catalyzing ozone
318 decay was relative to the surface acid–base properties of the oxides. Because of the
319 unsaturated state of surface electrons on the aluminum oxides, the surface would
320 adsorb water molecules. This behavior may result in the formation of surface
321 hydroxyl groups [25]. Surface hydroxyl groups play an important role in the
322 acid–base properties of aluminum oxides. It was thought that surface hydroxyl groups
323 made a significant contribution to the ability of aluminum oxides to catalyze ozone
324 decomposition. Nevertheless, some inorganic anions in the aqueous phase can be
325 adsorbed onto surfaces of oxides through ligand exchange with surface hydroxyl
326 groups, as shown in equation (6) [25]. If some inorganic anions inhibited the
327 catalyzed ozone decomposition, the activity of the aluminum oxides would be more
328 likely linked with the surface hydroxyl groups.



330 Kim et al. [30] had reported anions adsorption on hydrous oxides. In this paper, we

331 focused on sulfate and nitrate adsorption on aluminum oxides especially. Sulfate and
332 nitrate have different complexation affinities for Al^{3+} on the surface of aluminum
333 (hydroxyl) oxides. Figure 4A and Figure 4B showed adsorption process of sulfate and
334 nitrate on aluminum oxides. Results showed that both sulfate and nitrate could be
335 adsorbed on the surface of aluminum oxides. However, adsorption capacity of
336 aluminum oxides for sulfate and nitrate were different remarkably. For both sulfate
337 and nitrate, the adsorption capacity of HAO was the strongest among three aluminum
338 oxides. The adsorption capacity of AAO was the weakest. For outer sphere adsorption
339 mechanism, sulfate was adsorbed on the surface of aluminum oxide more easily.
340 Oppositely, adsorption capacity of nitrate on all aluminum oxides surface was fainter
341 than that of sulfate adsorbed on the surface of aluminum oxide. According to results
342 shown in Figure 4A and Figure 4B, more density of surface hydroxyl groups could
343 enhance adsorption capacity both for sulfate and nitrate adsorption on aluminum
344 oxides. Results shown in Figure 4A and Figure 4B confirmed that inorganic anions
345 were adsorbed on the surface of aluminum oxides by ligand exchange with surface
346 hydroxyl groups. Adsorption of sulfate and nitrate may result in decreasing of
347 surface hydroxyl groups. Figure 4A and Figure 4B also showed different initial
348 concentration anion adsorption. Adsorption of low concentration anion was very faint,
349 resulting in that ligand exchange of anions with surface hydroxyl groups was very
350 feebleness.

351

352 Figure 5 shows the impact of sulfate and nitrate on the rate constants of catalyzed

353 ozone decomposition in the presence of HAO, RAO and AAO. Nitrate and sulfate at
354 50 mmol L⁻¹ significantly inhibited ozone decomposition catalyzed by HAO, RAO
355 and AAO (Figure 4). Rate constants for ozone decomposition catalyzed by HAO,
356 RAO and AAO were 1.39 min⁻¹, 1.56 min⁻¹ and 1.80 min⁻¹, respectively. When
357 nitrate was present at 50 mmol L⁻¹, rate constants for HAO, RAO and AAO were 0.64
358 min⁻¹, 1.36 min⁻¹ and 1.73 min⁻¹. At 50 mmol L⁻¹ sulfate, rate constants for HAO,
359 RAO and AAO were 0.61 min⁻¹, 1.34 min⁻¹ and 1.63 min⁻¹. The effect of inhibition
360 was greatest for HAO and least for AAO. Sulfate had a greater ability than nitrate to
361 inhibit catalyzed ozone decomposition.

362

363 Sulfate and nitrate ions adsorb onto aluminum (hydroxyl) oxides via a complexation
364 reaction expressed in equation (6). Accordingly, the effect of sulfate and nitrate on
365 ozone decomposition catalyzed by the aluminum oxides was related to hydroxyl
366 groups on the surfaces of the catalysts. Surface hydroxyl groups on HAO, RAO and
367 AAO could be exchanged by the anions. Among the three aluminum oxides, HAO
368 possessed the highest density of surface hydroxyl groups but the effect of inhibition
369 by sulfate and nitrate anions was the greatest. For AAO, the opposite relationship was
370 observed. The hypothesis described above can be confirmed. As the affinity of sulfate
371 with surface hydroxyl groups was much stronger than that of nitrate, sulfate showed a
372 greater ability than nitrate to inhibit the ozone decomposition. The relationship
373 between the effectiveness of inhibition and the density of surface hydroxyl groups,
374 and the affinity of sulfate and nitrate for these surface hydroxyl groups, account for

375 the observation that surface hydroxyl groups on aluminum (hydroxyl) oxides play an
376 important role in catalytic ozone decomposition.

377

378 3.5 Effect of the presence of the ·OH-scavenger tert-butyl alcohol (TBA)

379 In recent years, many researchers considered that enhanced ozone transformation
380 into ·OH radicals occurred when ozone was decomposed in the presence of solid
381 catalysts. To determine whether ozone was transformed into ·OH radicals, tert-butyl
382 alcohol (TBA) was used as an effective scavenger as it does not react with ozone but
383 it does react with ·OH radicals (the second reaction rate constant of TBA with ·OH
384 radicals is $5.9 \times 10^8 \text{ (mol L)}^{-1} \text{ s}^{-1}$) [31]. Some inert compounds that have the potential
385 to terminate the chain reaction of ozone decomposition may be formed when TBA
386 reacts with ·OH radicals. [At the same time, TBA can not be adsorbed on the surface of](#)
387 [metal oxides, for physical-chemical property of TBA.](#) To investigate whether ozone
388 would be transformed into ·OH or not, further ozone decomposition experiments with
389 HAO, RAO and AAO were carried out in the presence of $0.675 \text{ mmol L}^{-1}$ TBA.
390 Figure 5 shows the apparent first order rate coefficients obtained from this series of
391 experiments. The rate coefficient decreased significantly compared with that obtained
392 in the corresponding experiment in the absence of TBA, regardless of the aluminum
393 (hydroxyl) oxide present (Figure 6). Results indicated that HAO, RAO and AAO
394 enhanced ozone decomposition primarily through the acceleration of the OH-radical
395 chain reaction in the liquid phase.

396

397 From the experiments on ozone decomposition using HAO, RAO and AAO in the
398 presence of TBA, the apparent first order kinetic constants k_{cata} and $k_{\text{cata+TBA}}$ were
399 calculated. The constant $(k_{\text{cata}} - k_{\text{cata+TBA}})$ denotes the inhibition effect of TBA on
400 ozone decomposition in the presence of HAO, RAO and AAO. For HAO, RAO and
401 AAO, $(k_{\text{cata}} - k_{\text{cata+TBA}})$ was 1.305, 1.191 and 1.083 min^{-1} , respectively. The density of
402 surface hydroxyl groups on each of the aluminum oxides was 8.83×10^{-5} , 3.17×10^{-5}
403 and $0.27 \times 10^{-5} \text{ mol}\cdot\text{m}^{-2}$ (Table 2). This indicates that the inhibition effect of TBA on
404 aluminum (hydroxyl) oxides was enhanced as the density of surface hydroxyl groups
405 increased. Therefore, surface hydroxyl groups account for enhanced ozone
406 decomposition in the presence of aluminum (hydroxyl) oxides.

407

408 3.6 Relationship between surface hydroxyl groups and catalytic activity of producing
409 hydroxyl radicals

410 From the above discussion, aluminum (hydroxyl) oxides exhibit greatest catalytic
411 activity when solution pH is close to PZC of the aluminum (hydroxyl) oxides. It was
412 also shown by experiments testing the effect of sulfate and nitrate that surface
413 hydroxyl groups played an important role in catalytic ozone decomposition in the
414 presence of HAO, RAO and AAO. Based on experiments testing of the effect of TBA,
415 it was confirmed that, during ozone decomposition, ozone was more effectively
416 transformed into OH radicals in the presence of HAO, RAO and AAO than when no
417 catalyst is present. Therefore, density of surface hydroxyl groups of aluminum
418 (hydroxyl) oxides may also be important in catalytic ozone decomposition. Further

419 experiments were carried out to investigate the relationship between density of surface
 420 hydroxyl groups of aluminum (hydroxyl) oxides and the concentration of $\cdot\text{OH}$ radicals
 421 transformed from ozone. The R_{ct} value expresses the ratio of $\cdot\text{OH}$ radical
 422 concentration to ozone concentration in ozonated water samples (see equations (7)
 423 and (8)) [32]. The R_{ct} value is constant during ozonation in any given type of water
 424 sample at any given ozone concentration. Here, the R_{ct} value was assumed to be
 425 constant for both non-catalytic and catalytic ozonation. This investigation used
 426 p-chlorobenzoic acid (pCBA) as a probe compound to determine the R_{ct} value both in
 427 non-catalytic and catalytic ozonation. The reaction rate constants of pCBA reacting
 428 with ozone and $\cdot\text{OH}$ are $k_{\text{O}_3/\text{pCBA}} \leq 0.15 \text{ (mol L)}^{-1} \text{ s}^{-1}$ [33] and $k_{\cdot\text{OH}/\text{pCBA}} = 5 \times 10^9 \text{ (mol}$
 429 $\text{L)}^{-1} \text{ s}^{-1}$ [34], respectively. The experiment results showed that **only less than 5% of**
 430 **pCBA was adsorbed on aluminum oxides**. Therefore, in the oxidation process, pCBA
 431 could react with $\cdot\text{OH}$ quickly. Using equations (7) and (8), the R_{ct} value, shown in
 432 Table 3, can be obtained for both non-catalytic and catalytic ozonation.

$$433 \quad R_{ct} = \frac{\int_0^t [\cdot\text{OH}] dt}{\int_0^t [\text{O}_3] dt} \quad (7)$$

$$434 \quad \ln \left\{ \frac{[\text{pCBA}]_t}{[\text{pCBA}]_0} \right\} = -k_{\cdot\text{OH}/\text{pCBA}} \int_0^t [\cdot\text{OH}] dt = -k_{\cdot\text{OH}/\text{pCBA}} R_{ct} \int_0^t [\text{O}_3] dt \quad (8)$$

435

436 The R_{ct} values in the presence of HAO, RAO and AAO were much higher than those
 437 found for ozonation without a catalyst. This means that aluminum (hydroxyl) oxides
 438 were able to transform ozone into OH radicals. The R_{ct} values increased as the density

439 of surface hydroxyl groups on the aluminum (hydroxyl) oxides increased. These
440 surface hydroxyl groups on the aluminum (hydroxyl) oxides were active in enhancing
441 the generation of hydroxyl radicals from aqueous ozone.

442

443 4. Conclusions

444 The results of this investigation provided evidence of the positive effect of aluminum
445 (hydroxyl) oxides on ozone transformation into $\cdot\text{OH}$ radicals. This effect depended
446 mainly on the dose of aluminum (hydroxyl) oxides, solution pH, inorganic anions and
447 the presence of tert-butyl alcohol. First order kinetics fitted perfectly to the ozone
448 decomposition reaction in the presence of HAO, RAO and AAO. The surface
449 acid–base properties of aluminum (hydroxyl) oxide played an important role in the
450 catalyzed ozone decomposition. The greatest catalytic effect on ozone decomposition
451 was observed when solution pH was close to PZC of the aluminum (hydroxyl) oxide.
452 The net surface charge of the aluminum (hydroxyl) oxide was favorable for catalyzed
453 ozone decomposition. The negative effect of inorganic anions on catalyzed ozone
454 decomposition indicated that surface hydroxyl groups of the aluminum (hydroxyl)
455 oxides contributed to ozone decomposition. The presence of tert-butyl alcohol
456 inhibited ozone decomposition catalyzed by aluminum (hydroxyl) oxide. This
457 indicated that ozone was transformed into hydroxyl radicals during catalyzed ozone
458 decomposition. By investigating the relationship between R_{ct} and the density of
459 surface hydroxyl groups on the aluminum (hydroxyl) oxide, it was confirmed that the
460 greater the density of surface groups the greater was the ability of the aluminum

461 (hydroxyl) oxide to transform ozone into hydroxyl radicals. Therefore, the surface
462 hydroxyl groups and acid–base properties of aluminum (hydroxyl) oxide play an
463 important role in catalyzed ozone decomposition.

464

465 Acknowledgements: This work was carried out with the financial support of The
466 National High Technology Research and Development Program of China
467 (2007AA06Z339) and the Program for New Century Excellent Talents in University
468 of China (NCET-04-0321).

469

470 References

471 [1] U. Von Gunten, *Water Res.* 37 (2003) 1443-1463.

472 [2] M. Skoumal, P.-L. Cabot, F. Centellas, C. Arias, R. M. Rodriguez, J. A. Garrido, E.
473 Brillas, *Appl. Catal. B- Environ.* 66 (2006) 228-240.

474 [3] C. L. Bianchi, C. Pirola, V. Ragaini, E. Selli, *Appl. Catal. B- Environ.* 64 (2006)
475 131-138.

476 [4] J. Ma, M. H. Sui, Z. L. Chen, N. W. Li, *Ozone Sci-Eng.* 26 (2004) 3-10.

477 [5] L. Zhao, J. Ma, Z.- Z. Sun, *Appl. Catal. B- Environ.* 79 (2008) 244-253.

478 [6] B. Legube, N. K. V. Leitner, Legube, B. and Leitner, N. K. V. *Catal. Today.* 53
479 (1999) 61-72.

480 [7] B. Kasprzyk-Hordern, P. Andrzejewski, A. Dabrowska, K. Czaczyk, J. Nawrocki,
481 *Appl. Catal. B- Environ.* 51 (2004) 51-66.

482 [8] J. Ma, N. J. D. Graham, *Water Res.* 34 (2000) 3822-3828.

- 483 [9] F. J. Beltrán, F. J. Rivas, R. Montero-de-Espinosa, *Appl. Catal. B- Environ.* 39
484 (2002) 221-231.
- 485 [10] M. Ernst, F. Lurot, J. C. Schrotter, *Appl. Catal. B- Environ.* 47 (2004) 15-25.
- 486 [11] B. Kasprzyk-Hordern, U. Raczek-Stanislawiak, J. Swietlik, J. Nawrocki, *Appl.*
487 *Catal. B- Environ.* 62 (2006) 345-358.
- 488 [12] B. Kasprzyk-Hordern, U. Raczek-Stanislawiak, J. Swietlik, J. Nawrocki, *Appl.*
489 *Catal. B- Environ.* 62 (2006) 345-358.
- 490 [13] T. Zhang, J. Ma, *J. Mol. Catal. A-Chem.* 279 (2008) 82-89.
- 491 [14] H. S. Park, T. M. Hwang, J. W. Kang, H. Choi, H. J. Oh, *Water Res.* 35 (2001)
492 2607-2614.
- 493 [15] P. C. C. Faria, J. J. M. Orfao, M. F. R. Pereira, *Appl. Catal. B- Environ.* 79 (2008)
494 237-243.
- 495 [16] M. Carbajo, F. J. Beltran, F. Medina, O. Gimeno, F. J. Rivas, *Appl. Catal. B-*
496 *Environ.* 67 (2006) 177-186.
- 497 [17] M. Sanchez-Polo, J. Rivera-Utrilla, *Appl. Catal. B- Environ.* 67 (2006) 113-120.
- 498 [18] H. Jung, H. Choi, *Appl. Catal. B- Environ.* 66 (2006) 288-294.
- 499 [19] M. Gruttadauria, L. F. Liotta, G. D. Carlo, G. Pantaleo, G. Deganello, P. L. Meo,
500 C. Aprile, R. Noto, *Appl. Catal. B- Environ.* 75 (2007) 281-289.
- 501 [20] P. M. Alvarez, F. J. Beltran, J. P. Pocostales, F. J. Masa, *Appl. Catal. B- Environ.*
502 72 (2007) 322-330.
- 503 [21] I. Udrea, C. Bradu, *Ozone Sci- Eng.* 25 (2003) 335-343.
- 504 [22] B. Kasprzyk-Hordern, M. Ziólek, J. Nawrocki, *Appl. Catal. B- Environ.* 46 (2003)

- 505 639–669.
- 506 [23] C. H. Ni, J. N. Chen, *Water Sci. Technol.* 43 (2001) 213–220.
- 507 [24] R. Gracia, J. Cortés, J. Sarasa, P. Ormad, J. L. Ovelleiro, *Ozone Sci- Eng.* 22
508 (2000) 461–471.
- 509 [25] W. Stumm, *Chemistry of the Solid–Water Interface*, Wiley & Sons Inc., New
510 York, 1992.
- 511 [26] M. Mullet, P. Fievet, A. Szymczyk, A. Foissy, J. C. Reggiani, J. Pagetti,
512 *Desalination* 121 (1999) 41–48.
- 513 [27] H. Tamura, A. Tanaka, K. Y. Mita, R. Furrichi, *J. Colloid Interf. Sci.* 209 (1999)
514 225–231.
- 515 [28] H. Bader, J. Hoigné, *Water Res.* 15 (1981) 449–456.
- 516 [29] H. N. Lim, H. Choi, T. W. Hwang, J. W. Kang, *Water Res.* 36 (2002) 219–229.
- 517 [30] F. H. Kim, P. Chaaralambos, O. James, *J. Colloid Interf. Sci.* 125 (1988) 717-726
- 518 [31] J. Stachelin, J. Hoigné, *Environ. Sci. Technol.* 19 (1985) 1206–1213.
- 519 [32] S. E. Michael, U. Von Gunten, *Ozone Sci- Eng.* 21 (1999) 239–260.
- 520 [33] C. C. D. Yao, W. R. Haag, *Water Res.* 25 761–773.
- 521 [34] P. Neta, L. M. Dorfman, *Advan. Chem. Serv.* 81 (1968) 222-230.

522

523

524

525

526

527 **Figure Caption**

528

529 Figure 1. Apparent first order kinetics plots for aqueous ozone decomposition.

530 Experimental conditions were: pH = 5.56; T=20 ± 1 °C; [O₃]₀ = 1.69 ± 0.02 mg L⁻¹;

531 catalyst dose (if applied): 0.2 g L⁻¹

532

533 Figure 2. Effects of catalyst dose on the apparent rate coefficient of ozone

534 decomposition. Experimental conditions were: pH = 5.56; T = 20 ± 1 °C;

535 [O₃]₀ = 1.69 ± 0.02 mg L⁻¹;

536

537 Figure 3. Changes in the reaction rate constant with aluminum (hydroxyl) oxides

538 minus the reaction rate constant without aluminum (hydroxyl) oxides at different pH

539 values. Experimental conditions were: T = 20 ± 1 °C; [O₃]₀ = 1.69 ± 0.02 mg L⁻¹;

540 catalyst dose = 0.2 g L⁻¹

541

542 Figure 4A. Adsorption of sulfate on the surface of aluminum oxides. Experimental

543 conditions were : T = 20 ± 1 °C; catalyst dose = 0.2 g L⁻¹; pH = PZC of aluminum

544 oxides (7.26, 8.26 and 9.40 for HAO, RAO and AAO, respectively)

545

546 Figure 4B. Adsorption of nitrate on the surface of aluminum oxides. Experimental

547 conditions were : T = 20 ± 1 °C; catalyst dose = 0.2 g L⁻¹; pH = PZC of aluminum

548 oxides (7.26, 8.26 and 9.40 for HAO, RAO and AAO, respectively)

549

550 Figure 5. Effects of inorganic anions on the apparent rate coefficient of ozone
551 decomposition. Experimental conditions were: $T = 20 \pm 1 \text{ }^\circ\text{C}$; $[\text{O}_3]_0 = 1.69 \pm 0.02$
552 mg L^{-1} ; $[\text{NO}_3^-]_0 = [\text{SO}_4^{2-}]_0 = 50 \text{ mmol L}^{-1}$; catalyst dose = 0.2 g L^{-1} ; pH = PZC of
553 aluminum oxides (7.26, 8.26 and 9.40 for HAO, RAO and AAO, respectively)

554

555 Figure 6. Effects of the presence and absence of TBA on the apparent rate coefficient
556 of ozone decomposition. Conditions of experiments: $T = 20 \pm 1 \text{ }^\circ\text{C}$; $[\text{O}_3]_0 = 1.69 \pm$
557 0.02 mg L^{-1} ; $[\text{TBA}]_0 = 0.675 \text{ mmol L}^{-1}$; catalyst dose = 0.2 g L^{-1} ; pH = PZC of
558 aluminum oxides (7.26, 8.26 and 9.40 for HAO, RAO and AAO respectively).

559

560